Interaction between shrub encroachment and water infiltration on a hillslope at the typical Steppe

Si-Yi Zhang [1, 2], Zhi-Hua Zhang [3], Bin He [1, 2], Zhi-Yun Jiang [4], Xiao-Yan Li [5, 6*]

[1] National-Regional Joint Engineering Research Center for Soil Pollution Control and Remediation in South China, Guangdong Key Laboratory of Integrated Agro-environmental Pollution Control and Management, Institute of Eco-environmental and Soil Sciences, Guangdong Academy of Sciences, Guangzhou 510650, China

[2] Guangdong-Hong Kong-Macao Joint Laboratory for Environmental Pollution and Control, Guangzhou 510650, China

[3] College of Forestry, Henan Agricultural University, Zhengzhou 450002, China

[4] School of Geography, South China Normal University, Guangzhou 510631, China

[5] State Key Laboratory of Earth Surface Processes and Resource Ecology, Faculty of Geographical Science, Beijing Normal University, Beijing 100875, China

[6] School of Natural Resources, Faculty of Geographical Science, Beijing Normal University, Beijing 100875, China

[*] Correspondence to: X.-Y. Li, School of Natural Resources, Faculty of Geographical Science, Beijing Normal University, Beijing 100875, China, E-mail:

19 xyli@bnu.edu.cn.

20

Interaction between shrub encroachment and water infiltration on a hillslope at the typical Steppe

Abstract The interaction between the surface hydrologic cycle and the shrub-encroached landscape at different slope positions remains poorly investigated. This study aims to explore the interaction between the water infiltration patterns affected by shrub encroachment at different hillslope positions. Soil water content and temperature were continuously measured at 10-min intervals at four or five depths under shrub patches and the grass matrix at four slope positions of a *Caragana microphylla* encroached hillslope from July 2009 to May 2013. The rainfall and meltwater infiltrations were estimated based on above data. Results showed that the rainfall infiltration ratios (IRs) at the grass matrix were as high as 0.78±0.08, except at the lower site, where it was only 0.47. The IRs of shrub patches increased from 0.38 at the top site to 0.77 at the lower site. The IRs were higher at the grass matrix than that at the shrub downslope edges at the top, upper, and middle sites of the hillslope due to the raised microtopography of the shrub mounds. However, at the lower site, IR was

higher at the shrub patch than that at the grass matrix than due to more upper slope runoff input and higher infiltration capacity at the shrub patches. The preferential flow was not an important factor influencing the redistribution of water resources on the slope. Snow and ice were blown up by wind and accumulated in the shrub patches and their lees resulted higher water input to the shrub patches than that in the grass matrix during snowy years. Shrub encroachment changed the microtopography, soil property under different canopy and slope positions, and further affected the surface hydrological processes. The feedbacks between shrub encroachment and water infiltration varied at different sites of the hillslope and affected the development of shrub patches.

Key words: Infiltration; rainfall; meltwater; shrub encroachment

1 Introduction

Shrub encroachment has been a worldwide phenomenon over more than 150 years in the arid or semi-arid regions, which refers to the increase in plant density, coverage and biomass of shrub in the grassland ecosystem

(Van Auken, 2000; Gibbens *et al*., 2005; Eldridge *et al*., 2011; D'Odorico *et al*., 2012). It is believed that erosion and climate change are the main causes of shrub encroachment (Sturm *et al*., 2001a; D'Odorico *et al*., 2012). Shrub encroachment redistributes light, heat, water, nutrients, and other resources, and changes net primary production, species diversity, etc. (Eldridge *et al*., 2011; Peng *et al*., 2014; Li *et al*., 2019; Zhou *et al*., 2019). The encroached vegetation interacts strongly with the environment (Rolo and Moreno, 2019; Turnbull and Wainwright, 2019), and their feedbacks would promote the encroachment and result a new longtime stable "climax community" (Thomas and Pittillo, 1987). The characteristics of the shrub patches were related to the soil water content and local precipitation, and with the increase of water resources, the optimal shrub coverage also increased (Valentin and D'Herbès, 1999; Zheng *et al*., 2015a).

Positive interactions between shrub encroachment and water resource of shrub patches were widely found. Li *et al*. (2013a) reported that soil water content at the depth of 60 cm under shrub patches was higher than that under grass matrix, which was related to their different $CaCO_3$ horizons characteristics. Higher infiltration depths and more preferential

flows under shrub patches were found in dying experiments with the same volume of dye solution (Zhang *et al*., 2012; Peng *et al*., 2013), which also revealed higher infiltration capacity under shrub patches (Peng *et al*., 2013; Li *et al*., 2013a). Shrub patches usually had lower runoff rates than grass land (Pierson *et al*., 2010; Munoz-Robles *et al*., 2011; Peng *et al*., 2013). Soliveres and Eldridge (2014) and Marquart *et al*. (2019) also reported that steady-state infiltration and sorptivity were greater under shrubs canopies than those in open areas, and positive effects of shrub were ascribed to the reduction of trampling from livestock. Hu *et al*. (2015, 2018) found that soil macroporosity and macropore volume in shrubs patches were higher than those in grass patches, and they increased with increasing shrub root network density. Thus, it was speculated that water could transport to the deeper soil layers in shrub patches (Hu *et al*., 2015; 2018). The root channels of the shrub were thought to be preferential pathways of water movement and could let water reach deep soil layer (Martinez-Meza and Whitford, 1996; Wang *et al*., 2007; Li *et al*., 2009; Zhang *et al*., 2012). On the other side, Rossi and Ares (2017) modeled the water fluxes between inter-patches and shrub mounds and found that shrub mounds could

directly obtain more water resource from the rain, but overland flow from the inter-patches could only reach the border of the shrub mounds and could not route onto the shrub mounds, and no ponded-water inundates the mound. So, as most of the former infiltration and runoff studies were conducted under artificial condition, how the infiltration in shrub patches act under natural precipitation, and whether the effects are positive in different parts of the shrub patches (center and edge) as well as on different positions of a hillslope were still unclear.

The snow can be an important soil water input and influence soil water infiltration and storage (Stewart *et al*., 2004; Murray and Buttle, 2005). Meltwater can form macropore flow in rooted soil, which effectively storages water for plants (Newman *et al*., 2004). Snow melting in arid and semi-arid areas can improve soil moisture, create conditions for seed germination and growth, and even have a profound impact on the water competition within and between species and on the spatial pattern of vegetation (Li *et al*., 2006). The redistribution of water resource will affect the productivity and distribution of vegetation (Weltzin *et al*., 2003). In the Arctic, deciduous shrubs obtained more water from snow than grass in the

111 growing season, and this meltwater-focused feedback loop could explain
112 the shrub expansion (Jespersen *et al.*, 2018). In addition, shrub
113 encroachments have greatly changed the landscape pattern of grassland
114 ecosystem, local radiation balance, physical characteristics and structures
115 of snow cover (Murray and Buttle, 2003), and further changed the local
116 microclimate, runoff, and soil water conditions (Wilcox *et al.*, 2003; Li *et*
117 *al.*, 2006). The biomass and height of shrub patches were higher than those
118 of the grass inter-patches in seriously disturbed conditions (Peng *et al.*,
119 2013). Thus, shrub patches could trap and retain more snow and meltwater
120 resource (Sturm *et al.*, 2001b; Tape *et al.*, 2006; Myers-Smith *et al.*, 2011;
121 Yan *et al.*, 2019). But how these effects perform on different slope position
122 and under different snow level in the north China need more investigation.
123 Therefore, the aims of this study were to (a) investigate the infiltration
124 characteristics under natural rainfall at different sites of a slope with shrub
125 encroachment, and (b) evaluate the effects of the meltwater infiltration on
126 water resources of shrub patches. This study would explore the
127 relationships between the development of the encroached shrub patches
128 and the infiltration pattern at different sites of the slope. The results are of

great significance to explain the spatial distribution characteristics of encroached shrub and predict its future development trend under changing climate background.

2 Methods and Materials

2.1 Study site

This study was carried out at the Taipus Banner, Inner Mongolia, China. This area belongs to the typical Eurasian Steppe and has continental temperate semiarid climate. Its mean annual temperature and mean annual precipitation are 1.6 °C and 392 mm, respectively (Li *et al.*, 2013a). The hottest month is July (17.8 °C on average) and the coldest month is January (-17.6 °C on average). 65% of precipitation occurs from July to September. Annual pan evaporation reaches 1900 mm on average. The average annual wind velocity is 3 - 5 m s^{-1} and the annual period of force-seven wind and above is 20 - 80 d, mainly occurring in spring and winter. The annual frost-free period is around 100 d, from late May or early June to early September. The zonal soils are chestnut soil and light chestnut soil, which are equivalent to Calcicorthic Aridisol according to USDA Soil Taxonomy.

147 Soil textures were mainly sand and sandy loam. The dominant plant species
148 were *Stipa krylovii* Roshev., *Cleistogenes squarrosa* (Trin.) Keng,
149 *Artemisia frigida* Willd., and *Leymus chinensis* (Trin.) Tzvel (Qiu *et al.*,
150 2011). *Caragana microphylla* Lam expansion increased during recent
151 decades in this region. It is estimated the area of *C. microphylla* encroached
152 grassland amounted to more than 5.1×10^6 ha (Zhang *et al.*, 2006), and the
153 coverage of this shrub can reach 40.1% (Peng *et al.*, 2013).

154 One *C. microphylla* encroached hillslope was selected for this study
155 (Figure 1). This west slope is 128 m in length and has an average slope
156 gradient of 12.5% (Li *et al.*, 2013a). This slope was evenly divided into
157 four sites from the ridge to the valley: the top, upper, middle, and lower
158 sites (Figure 1). The sizes of shrub patches were 3.93, 5.86, 5.84, and 7.68
159 m^2 at the top, upper, middle, and lower sites of the slope, respectively, and
160 their canopy heights were 0.43, 0.55, 0.47, and 0.41 m, respectively (Li *et*
161 *al.*, 2013a). The above ground biomasses of the shrub patches at four sites
162 were 343, 400, 403, and 428 g m^{-2} from top to lower sites, respectively,
163 while that of the grass matrix were 108, 140, 141, and 185 g m^{-2},
164 respectively (Li *et al.*, 2013a). The canopy coverage of shrub patches was

93-95%, and that of the grass matrix is 68-75% in the peak season (Li *et al.*, 2013a). The rooting depths were 60 - 70 cm and 20 - 25 cm at the shrub patches and at the grass matrix, respectively (Li *et al.*, 2013a).

<Figure 1>

2.2 Soil water content and temperature measurement

Eight soil profiles were instrumented at the top, upper, middle, and lower sites of the slope, two for each site (Li *et al.*, 2013a): one at the downslope edge of a *C. microphylla* shrub patch, and the other at the grass matrix, about 1 m from the upslope edge of the *C. microphylla* shrub patch (Figure 1). Five ECH2O 5TE sensors (Decagon Devices, Pullman, Washington, USA) were installed in each soil profile to monitor soil water content (θ, m^3 m^{-3}) and soil temperature (T_s, °C) at the soil depths of 10, 20, 40, 60, and 100 cm. Except for the middle site, the ECH2O 5TE sensors was replaced by Decagon Drain Gauges at the100 cm depth to detect soil water drainage (Figure 1). A total of thirty-eight ECH2O 5TE sensors were installed at four sites of the slope. All data of θ and T_s, as well as drainage, if available, at each profile were logged into a 5-channel Decagon's Em50 data logger at 10-min intervals. These ECH2O 5TE sensors can provide

accurate, precise and continuous measurements, with the accuracy of ±0.012 m^3 m^{-3} for moisture, ±0.3°C for soil temperature (Czarnomski *et al.*, 2005; Li *et al.*, 2013a). The experiments started on June 8, 2009, and data since July 1, 2009, or later was used considering the disturbance of profiling and setting of the sensors (Table 1). The monitoring last to May 16, 2011, at the top, upper, and lower sites, while at the middle site, it last to May 21, 2013 (Table 1).

<Table 1>

2.3 Meteorological observations

A Dynamet weather station (Dynamax Inc., Houston, TX, USA) was set up to measure the meteorological data at the center of the slope. Rainfall was measured using a tipping bucket rain gauge (Model TE525, Campbell Scientific, Logan, UT, USA). Air temperature (T_a, °C) was recorded using a temperature and humidity probe (Model CS500, Campbell Scientific, Logan, UT, USA) at 2 m above the ground. Wind speed and direction were detected by a windvane and anemovane (Model 03001, RM Young Co.,

Traverse City, MI, USA), positioned at 3 m above the ground. Snowfall data were obtained from the Weather Station of Taipus Banner (41.88°N, 115.27°E,1468.9 m *a.s.l.*).

2.4 Infiltration ratios estimation

The rain events were discretized by assuming a minimum interevent time of 24 h. Soil water storage (*SWS*, mm) of a 1 m profile was calculated as:

$$SWS = \sum_{k=1}^{n} \theta_k D_k \quad (1)$$

where θ_k (m^3 m^{-3}) represents θ measured by 5TE seniors at soil layer k, D_k is the depth of θ_k represents (mm). n represents the number of the 5TE sensors at the 1 m profile. At the top, upper, and lower sites, n = 5, and D_k = 150, 150, 200, 300, and 200 mm for k = 1, 2, 3, 4, and 5, respectively; while at the middle sites, n = 4, and D_k = 150, 150, 200, and 500 mm for k = 1, 2, 3, and 4, respectively. Infiltration amounts (I, mm) in a rainfall event was estimated as the maximum difference of *SWS* before and after the rainfall event (before the next rainfall). The infiltration ratio (*IR*) was estimated as the slopes of the linear regression of I against rainfall amounts at the experimental period (Zhang and Li, 2018).

2.5 Preferential flow detection

The preferential flow (PF) during natural precipitation were detected by the response sequences of θ of different soil layers. Only events with over 1 mm of rainfall were analyzed considering that small rainfall could not infiltrate deeper than the first sensor. The θ was examined and thought to have response to rainfall if its increase was over 0.01 m^3 m^{-3} during an rainfall event due to the precision and noise levels of the sensors was 0.01 m^3 m^{-3} (Graham and Lin, 2011). If a deeper sensor responds before, or simultaneously with a shallower sensor, or when a shallower sensor does not respond, it was thought that preferential flow happened at this profile in this event (Graham and Lin, 2011; Hopkins *et al*., 2016).

2.6 Meltwater infiltration estimation

When the soil was frozen, θ decreased as soil water transferred into ice. During the frozen period, soil water was protected from evaporation. After thawed, θ can nearly return to the same level before soil was frozen. Basing on this assumption and ignoring the evaporation during this period, meltwater infiltration was calculated as the differences of the maximum *SWS* before the first rain in a spring (after thawing) and the *SWS* just before

237 the soil freezing in the last winter (Figure 2).

238

239 <Figure 2>

240

241 # 3 Results

242 ## 3.1 Precipitation and wind characteristics

243 Characteristics of rainfalls in the experimental area during the nearly
244 four years (from July 1, 2009, to May 21, 2013) were given in Figure 3. A
245 total of 144 rainfall events (excluding snowfall) occurred in nearly four
246 years, accumulating 904.71 mm of rainfall. They were mainly short small
247 storms, with 46 (31.94%) rainfall events smaller than 1 mm, and 96
248 (66.67%) rainfall events not higher than 5 mm. Rainfalls larger than 10 mm
249 only accounted for 13.19% of all rainfall events but accounted for 65.52%
250 of the rainfall amount. The maximum rainfall was 59.69 mm recorded
251 during September 15 ~ 18, 2010. The rainfall intensity ranged from 0.02 to
252 13.20 mm h^{-1}. The maximum 10 - min intensity ranged from 0.20 to 73.15
253 mm h^{-1}, with only 10.42% of which larger than 10 mm h^{-1}, and only one of
254 them was larger than the 63.23 mm h^{-1} infiltration rate of grass matrix at

suctions of 0.5 mm (Li *et al.*, 2013a). The snowfalls were 39.5, 49.5, 29.1, and 45.1 mm during the winter and spring of 2009-2010, 2010-2011, 2011-2012, and 2012-2013, respectively. The wind in winter and spring were mainly from W, WSW, SW, and SSW, and their speeds mainly ranged from 2 - 10 m s^{-1} with an average speed of 5.2 m $s^{-1}$and a maximum of 18.8 m s^{-1} (Figure 4).

<Figure 3>

<Figure 4>

3.2 Rainfall infiltrations

Rainfall infiltrations varied at different slope position and under different land covers. At the top, upper, and middle grass matrix, *IRs* were as high as 0.78±0.08, while at the lower grass matrix, it was only 0.47 (Figure 5). The *IRs* of shrub patches increased from 0.38 at the top site to 0.77 at the lower site (Figure 5).

The yearly total infiltration showed similar results to the *IRs* (Figure 6). At the top and upper sites, the grass matrix had higher yearly total

273 infiltration than shrub patches, with higher differences at the top site than
274 at the upper site. The yearly total infiltration at the lower shrub patch was
275 higher than that at the lower grass matrix.

276 The yearly infiltrations in 2010 were available at all sites with a
277 minimum of 69.4 mm at the top shrub patch and a maximum of 194.5 mm
278 at the upper grass matrix. In 2011 and 2012, the whole year infiltrations
279 were available at the middle sites. The yearly infiltration of 2011 was 212.4
280 mm at the middle shrub patch, the maximum of all sites in the whole
281 experimental period, and much higher than the 138.3 mm at the middle
282 grass matrix. In 2012, the yearly infiltration at the middle shrub patch was
283 123.1 mm, lower than that of 155.6 mm at the middle grass matrix. From
284 the 2010 to 2012, the yearly infiltration at the middle shrub patch was 152.1
285 ±52.2 mm, insignificantly higher than that at the middle grass matrix,
286 143.4±10.5 mm, basing on the 2-tailed paired sample T test (p=0.818).

287

288 <Figure 5>

289 <Figure 6>

290

PF ratios were only 4.1% and 2.4% at grass matrix and shrub patches, respectively (Table 1) with total 19 PF events recorded. Most of PF events were recorded at 60 and 40 cm at the grass matrix and shrub patches, respectively (Table 1). Grass matrix had higher PF ratios than the shrub patches. There were no PF events recorded at the top sites. At the grass matrix, the most PF events were recorded at the middle site, followed by the lower site; while at the shrub patches, the highest PF ratios were recorded at the middle site. All these 19 PF events came from different rainfall events, with the ranges of rainfall depth, rain intensity, and the maximum 10 - min rainfall intensities of 1 - 37.85 mm, 0.05 - 9.60 mm h^{-1}, and 1.20 - 57.90 mm h^{-1}, respectively.

3.3 Meltwater infiltrations

The meltwater infiltrations varied in different years (Figure 7). In the winters of snowless years (2009 - 2010 and 2011 - 2012), the meltwater infiltration was low, no more than 5 mm except at the middle grass matrix site (6.3 mm), and no infiltration at the shrub patches at both the upper and lower sites. In these years, the meltwater infiltration was higher at the grass matrix than that at the shrub patches. While at the snowy years, the

meltwater infiltration was relatively higher, ranging from 5.17 to 12.94 mm in the spring of 2011 (Figure 7). In these snowy years, the meltwater infiltration was higher in the shrub patches than that in the grass matrix, except for the middle site in the winter of 2010-2011.

Especially, meltwater infiltration was quite high at the middle grass matrix and shrub patch in the spring of 2013 (Figure 8). The soil temperature dropped chronically below 0 °C from 1 a.m. and 6 a.m., November 13, 2012 at the middle grass matrix and the shrub patch, respectively. Before the soil froze in the middle grass and shrub sites, their *SWS*s were 137.6 and 102.91, respectively. After the soil was frozen, no rainfalls were recorded. As soil water transferred to ice, the liquid θ successively reduced from 10 cm to 60 cm depth , and the liquid *SWS* of the whole profile gradually reduced. The positive soil temperature at 10 cm depth was first recorded at 4 p.m. March 7, 2013, at the middle grass matrix, while at the middle shrub patch, it was at 12 a.m. March 8, 2013. During these two days, the air temperature increased rapidly and reached 12.0 °C at 3 p.m. After the soil temperature at 10 cm depth stride over the freezing point, the θ increased quickly and successively at each soil layer. The liquid

SWS of the whole profile bulged rapidly at both middle grass and shrub sites, reaching 224.4 and 232.7 mm at 7 p.m. March 8, 2013, respectively. The meltwater infiltration reached 86.8 mm and 129.8 mm at the middle grass and shrub sites, respectively.

<Figure 7>

<Figure 8>

4 Discussions

Lower *IRs* and PF ratios were found at the downslope edge of shrub patches than that at the grass matrix except for the lower site. This can be related to the slope topography and position where the 5TE sensors were installed. The shrub patches form mounds and are raised microtopography (Figure 1 and Figure 9). This is because that shrub prevents the ground from livestock trampling and erosion, and on other side accumulates wind and water sediment (Stavi *et al*., 2008; Lu *et al*., 2019; Yang *et al*., 2019). In this condition, the water flow from upslope would first reach the upslope edge of shrub mounds, and water flow would mainly infiltrate there or

345 bypass the of shrub mounds, which results less water source for the
346 downslope edge of the shrub patches. The 5TE sensors were installed at
347 the downslope edge of the shrub patches and they had the relatively higher
348 slope gradients (Stavi *et al*., 2008), which had higher possibility to generate
349 more runoff and reduce water infiltration. Therefore, the microtopgraphy
350 of shrub patches resulted that the downslope edge of the shrub patches
351 generated more local runoff and stored less water source from upslope.
352 This would be the main reason for the low *IR* there, which is consistent
353 with the result of Li *et al*. (2013b), who reported lower soil moisture at the
354 downslope edges of shrub patches comparing to that at the upslope edges
355 after rainfalls.

356 Higher *IR* was found at the downslope edge of shrub patches at the
357 lower site. This is because there was more runoff from the upslopes and
358 there was plenty of water flowing over or around the shrub mound to gather
359 at the downslope edge of the shrub patches. The upslope runoff would form
360 ponding water and increase their infiltration as the shrub patches had higher
361 infiltration rates (Li *et al*., 2013a) and deeper infiltration depth under water
362 ponding conditions (Zhang *et al*., 2012; Peng *et al*., 2013). In addition, the

363 shrub patch at the lower site had the highest aboveground biomass and root
364 depth, higher soil organic matter (Li *et al*., 2013a), and more sand and silt
365 (Zhang *et al*., 2019), which could generate more macropores and increase
366 water infiltration (Hu *et al*., 2015; 2018). However, the lower grass matrix
367 site had the lowest total infiltration among the four grass matrix sites. This
368 can be explained by more clay deposited on the lower grass matrix, which
369 could block the macropores and reduce infiltration capacity (Li *et al*.,
370 2013a).

371 The PF ratios at the experimental sites were no more than 5%, much
372 lower than the 17 to 54% at the Shale Hills Critical Zone reported by
373 Graham and Lin (2011). This may be related to their different soil types
374 and rainfall characteristics. The soil of Shale Hills Critical Zone was
375 formed by shale residuum and colluvium, which were not very well
376 developed due to the cold weather and contained a lot of rock which
377 increased the formation of PF. While the soil at our experimental sites was
378 chestnut soil and light chestnut soil, developed from aeolian sediment, and
379 had relative uniform texture throughout the profile. This would not be
380 beneficial to the formation of PF. Another reason is that there were few

heavy rainfall events in the experimental sites. The most influential factors of PF were water input amounts and peak input intensity (Hopkins *et al*., 2016). The PF usually occurrences when the water input over a threshold (Mcgrath *et al*., 2010). As showed in Figure 3, rainfalls larger than 10 mm only accounted for 13.19% of all rainfall events. The more aboveground biomass at the shrub patches(Peng *et al*., 2013) also intercepted more rainfall and reduced the net rainfall reached the ground (Zhang *et al*., 2018). The lower PF ratios of shrub patches can be connected to their low *IRs*, which equaled to their lower water input.

Meltwater infiltration is also from two sources: One is the snow and ice on the site, and the other is the runoff from the upslope. In the snowless years, the meltwater flow was weak and bypassed the shrub mounds. Thus, the grass matrix could get meltwater from the upslope while the downslope edge of shrub mounds could not get meltwater, resulting in lower meltwater infiltration at the downslope edge of shrub compared with the grass matrix. So, the meltwater infiltration was lower at the downslope edge of shrub than at the grass matrix. On the contract, in the snowy years, snow and ices were trapped and retained on the shrub patches and at the lee side. The

399 strong meltwater flow from the upslope and the top of the shrub mound
400 could reach the downslope edge of the shrub patch and then increase the
401 meltwater infiltration there (Figure 9). Due to the higher infiltration
402 capacity of the shrub patches, they had higher meltwater infiltration. In
403 general years, the meltwater infiltration did not exceed 15 mm, which could
404 only be about 20 mm of rainfall infiltration. However, in some separate
405 years, snow was heavy and the shrub patches retained a lot of snow and ice.
406 Additionally, if the weather in spring warm up rapidly, the snow and ice
407 stack would melt rapidly and generate flood over the slope (Figure 9).
408 Compared with most years, this meltwater flow could infiltrate more
409 (Figure 7) and reach the soil layer of 60 cm or deeper (Figure 8).

410 The meltwater infiltration increased the θ in the spring. In the snowless
411 years, θonly weakly increased and decreased quickly below the level
412 before the soil was frozen in the last year. The effect of the meltwater, the
413 period when θ in spring (before the first rain) is higher than θ before frozen
414 in the last winter, was usually less than 10 days. However, at the snowy
415 years, θstrongly increased and the effect of θ was usually longer than 20
416 days and lasted to the start of vegetation greenup. Especially, in the spring

of 2013, the θ at the middle grass and shrub sites was higher than that before frozen till the end of the experiment, lasting more than 73 days. The increased θ of meltwater water infiltration was an important soil water resource in the semiarid region, which had a great influence on the sprout and regreen of vegetation there (Stewart *et al.*, 2004; Barrere *et al.*, 2018). The heavy and deep meltwater infiltration in the spring of 2013 would even have a significant impact on the growth of local vegetation (Zheng *et al.*, 2015b).

<Figure 9>

5 Conclusions

Shrub patches could retain more water resources at the lower site of the hillslope and meltwater can be an important water resource of the shrub patches during snowy years. The preferential flow might not be an important factor influencing the redistribution of water resources on the slope. The downslope edge of the shrub patches retained lower rain water resources than the grass matrix at the top, upper, and middle sites. The

435 downslope edge of shrub patches at the middle, upper, and top sites would
436 degrade due to less water resource, and the upslope edge of shrub patches
437 would expand toward the top of the slope. However, as shrub patches
438 expand toward the top, the runoff resources and their *IRs* declined. Thus,
439 the size of the shrub patch would stay steady when the degradation and
440 expansion are balanced. The shrub patches at the lower site would expand
441 in all direction and expand to larger sizes as they could retain more water
442 resources.
443

444 **Data availability.**

445 No data sets were used in this article.
446

447 **Author contributions.**

448 XYL and SYZ had the initial idea of the paper and created the storyline.
449 XYL, SYZ, ZHZ, and ZYJ carried out the experiments. SYZ analyzed the
450 data. SYZ, ZHZ, and ZYJ wrote the initial manuscript. DF, BH and YCZ
451 reviewed and improved the text upon the initial version.
452

Competing interests.

The authors declare that they have no conflict of interest.

Acknowledgements

This work was supported by the National Natural Science Foundation of China (Grant Nos. NSFC 41977010 and 41930865), the Guangdong Basic and Applied Basic Research Foundation (Grant No. 2019A1515010628), the GDAS Special Project of Science and Technology Development, China (Grant Nos. 2020GDASYL-20200102013 and 2020GDASYL-20200301003).

References

Barrere M, Domine F, Belke-Brea M, Sarrazin D. 2018. Snowmelt Events in Autumn Can Reduce or Cancel the Soil Warming Effect of Snow−Vegetation Interactions in the Arctic. Journal of Climate 31(23): 9507-9518. DOI: 10.1175/JCLI-D-18-0135.1

Czarnomski N, Moore GW, Pypker TG, Licata J, Bond BJ. 2005. Precision and accuracy of three alternative instruments for measuring soil water content in two forest soils of the Pacific Northwest. Canadian Journal of Forest Research 35(8): 1867-1876. DOI: 10.1139/x05-121

D'Odorico P, Okin GS, Bestelmeyer BT. 2012. A synthetic review of feedbacks and drivers of shrub encroachment in arid grasslands. Ecohydrology 5(5): 520-530. DOI: 10.1002/eco.259

Eldridge DJ, Bowker MA, Maestre FT, Roger E, Reynolds JF, Whitford WG. 2011. Impacts of shrub encroachment on ecosystem structure and functioning: towards a global synthesis. Ecology Letters 14(7): 709-722. DOI: 10.1111/j.1461-0248.2011.01630.x

Gibbens RP, Mcneely RP, Havstad KM, Beck RF, Nolen B. 2005. Vegetation changes in the Jornada Basin from 1858 to 1998. Journal of Arid Environments 61(4): 651-668.

Graham CB, Lin HS. 2011. Controls and Frequency of Preferential Flow Occurrence: A 175-Event Analysis. Vadose Zone Journal 10(3): 816-831. DOI: 10.2136/vzj2010.0119

Hopkins I, Gall H, Lin H. 2016. Natural and anthropogenic controls on the frequency of preferential flow occurrence in a wastewater spray irrigation field. Agricultural Water Management 178: 248-257. DOI: 10.1016/j.agwat.2016.09.011

Hu X, Li X, Guo L, Liu Y, Wang P, Zhao Y, Cheng Y, Lyu Y, Liu L. 2018. Influence of shrub roots on soil macropores using X-ray computed tomography in a shrub-encroached grassland in Northern China. Journal of Soils and Sediments. DOI: 10.1007/s11368-018-2218-6

Hu X, Li Z, Li X, Liu Y. 2015. Influence of shrub encroachment on CT-measured soil macropore characteristics in the Inner Mongolia grassland of northern China. Soil and Tillage Research 150: 1-9. DOI: 10.1016/j.still.2014.12.019

Jespersen RG, Leffler AJ, Oberbauer SF, Welker JM. 2018. Arctic plant ecophysiology and water source utilization in response to altered snow: isotopic (delta O-18 and delta H-2) evidence for meltwater subsidies to deciduous shrubs. Oecologia 187(4SI): 1009-1023. DOI: 10.1007/s00442-018-4196-1

Li H, Shen H, Zhou L, Zhu Y, Chen L, Hu H, Zhang P, Fang J. 2019. Shrub encroachment increases soil carbon and nitrogen stocks in temperate grasslands in China. Land Degradation & Development 30(7): 756-767. DOI: 10.1002/ldr.3259

Li J, Zhao C, Zhu H, Wang F, Wang L, Kou S. 2006. Multi scale spatial heterogeneity of soil water in Haloxylon ammodendron woodland after snowmelt. Chinese Science: Part D 36(A02): 45-50. (In Chinese with English abstract)

Li X, Hu X, Zhang Z, Peng H, Zhang S, Li G, Li L, Ma Y. 2013b. Shrub Hydropedology: Preferential Water Availability to Deep Soil Layer. Vadose Zone Journal 12(4): 1-12. DOI: doi:10.2136/vzj2013.01.0006

Li X, Zhang S, Peng H, Hu X, Ma Y. 2013a. Soil water and temperature dynamics in shrub-encroached grasslands and climatic implications: Results from Inner Mongolia steppe ecosystem of north China. Agricultural and Forest Meteorology 171-172: 20-30.

Li XY, Yang ZP, Li YT, Lin H. 2009. Connecting ecohydrology and hydropedology in desert shrubs: stemflow as a source of preferential flow in soils. Hydrology and Earth System Sciences 13(7): 1133-1144.

Lu R, Liu Y, Jia C, Huang Z, Liu Y, He H, Liu B, Wang Z, Zheng J, Wu G. 2019. Effects of mosaic-pattern shrub patches on runoff and sediment yield in a wind-water erosion crisscross region. Catena 174: 199-205. DOI: https://doi.org/10.1016/j.catena.2018.11.022

Marquart A, Eldridge DJ, Travers SK, Val J, Blaum N. 2019. Large shrubs partly compensate negative effects of grazing on hydrological function in a semi-arid savanna. Basic and Applied Ecology 38: 58-68. DOI: 10.1016/j.baae.2019.06.003

Martinez-Meza E, Whitford WG. 1996. Stemflow, throughfall and channelization of stemflow by roots in three Chihuahuan desert shrubs. Journal of Arid Environments 32(3): 271-287. DOI: doi: 10.1006/jare.1996.0023

Mcgrath GS, Hinz C, Sivapalan M, Dressel J, Puetz T, Vereecken H. 2010. Identifying a rainfall event threshold triggering herbicide leaching by preferential flow. Water Resources Research 46(W02513). DOI: 10.1029/2008WR007506

Munoz-Robles C, Reid N, Tighe M, Briggs SV, Wilson B. 2011. Soil hydrological and erosional responses in patches and inter-patches in vegetation states in semi-arid Australia. Geoderma 160(3-4): 524-534. DOI: 10.1016/j.geoderma.2010.10.024

Murray CD, Buttle JM. 2003. Impacts of clearcut harvesting on snow accumulation and melt in a northern hardwood forest. Journal of Hydrology 271(1): 197-212. DOI: https://doi.org/10.1016/S0022-1694(02)000352-9

524 Murray CD, Buttle JM. 2005. Infiltration and soil water mixing on forested and harvested slopes during
525 spring snowmelt, Turkey Lakes Watershed, central Ontario. Journal of Hydrology 306(1): 1-20. DOI:
526 https://doi.org/10.1016/j.jhydrol.2004.08.032
527 Myers-Smith IH, Forbes BC, Wilmking M, Hallinger M, Lantz T, Blok D, Tape KD, Macias-Fauria M,
528 Sass-Klaassen U, Lévesque E, Boudreau S, Ropars P, Hermanutz L, Trant A, Collier LS, Weijers S,
529 Rozema J, Rayback SA, Schmidt NM, Schaepman-Strub G, Wipf S, Rixen C, Ménard CB, Venn S,
530 Goetz S, Andreu-Hayles L, Elmendorf S, Ravolainen V, Welker J, Grogan P, Epstein HE, Hik DS.
531 2011. Shrub expansion in tundra ecosystems: dynamics, impacts and research priorities.
532 Environmental Research Letters 6(4): 45509. DOI: 10.1088/1748-9326/6/4/045509
533 Newman BD, Wilcox BP, Graham RC. 2004. Snowmelt-driven macropore flow and soil saturation in a
534 semiarid forest. Hydrological Processes 18(5): 1035-1042.
535 Peng H, Li X, Li G, Zhang Z, Zhang S, Li L, Zhao G, Jiang Z, Ma Y. 2013. Shrub encroachment with
536 increasing anthropogenic disturbance in the semiarid Inner Mongolian grasslands of China. Catena
537 109(1): 39-48. DOI: 10.1016/j.catena.2013.05.008
538 Peng H, Li X, Tong S. 2014. Advance in shrub encroachment in arid and semiarid region. Acta
539 Prataculturae Sinica 23(2): 313-322. (In Chinese with English abstract) DOI: 10.11686/cyxb20140237
540 Pierson FB, Williams CJ, Kormos PR, Hardegree SP, Clark PE, Rau BM. 2010. Hydrologic Vulnerability
541 of Sagebrush Steppe Following Pinyon and Juniper Encroachment. Rangeland Ecology &

Management 63(6): 614-629. DOI: 10.2111/REM-D-09-00148.1

Qiu GY, Xie F, Feng YC, Tian F. 2011. Experimental studies on the effects of the "Conversion of Cropland to Grassland Program" on the water budget and evapotranspiration in a semi-arid steppe in Inner Mongolia, China. Journal of Hydrology 411(1-2): 120-129. DOI: doi: 10.1016/j.jhydrol.2011.09.040

Rolo V, Moreno G. 2019. Shrub encroachment and climate change increase the exposure to drought of Mediterranean wood-pastures. Science of the Total Environment 660: 550-558. DOI: https://doi.org/10.1016/j.scitotenv.2019.01.029

Rossi MJ, Ares JO. 2017. Water fluxes between inter-patches and vegetated mounds in flat semiarid landscapes. Journal of Hydrology 546: 219-229. DOI: https://doi.org/10.1016/j.jhydrol.2017.01.016

Soliveres S, Eldridge DJ. 2014. Do changes in grazing pressure and the degree of shrub encroachment alter the effects of individual shrubs on understorey plant communities and soil function? Functional Ecology 28(2SI): 530-537. DOI: 10.1111/1365-2435.12196

Stavi I, Ungar ED, Lavee H, Sarah P. 2008. Surface microtopography and soil penetration resistance associated with shrub patches in a semiarid rangeland. Geomorphology 94(1): 69-78. DOI: https://doi.org/10.1016/j.geomorph.2007.05.008

Stewart IT, Cayan DR, Dettinger MD. 2004. Changes in Snowmelt Runoff Timing in Western North America under a `Business as Usual' Climate Change Scenario. Climatic Change 62(1): 217-232. DOI:

10.1023/B:CLIM.0000013702.22656.e8

Sturm M, Holmgren J, Mcfadden JP, Liston GE, Chapin Iii FS, Racine CH. 2001b. Snow–shrub interactions in Arctic tundra: a hypothesis with climatic implications. Journal of Climate 14(3): 336-344.

Sturm M, Racine C, Tape K. 2001a. Increasing shrub abundance in the Arctic. Nature 411(6837): 546-547. DOI: 10.1038/35079180

Tape K, Sturm M, Racine C. 2006. The evidence for shrub expansion in Northern Alaska and the Pan-Arctic. Global Change Biology 12(4): 686-702. DOI: 10.1111/j.1365-2486.2006.01128.x

Thomas RB, Pittillo JD. 1987. Invasion of fagus-grandifolia ehrh into a rhododendron-catawbiense michx heath bald at craggy gardens, north-Carolina. Castanea 52(3): 157-165.

Turnbull L, Wainwright J. 2019. From structure to function: Understanding shrub encroachment in drylands using hydrological and sediment connectivity. Ecological Indicators 98: 608-618. DOI: https://doi.org/10.1016/j.ecolind.2018.11.039

Valentin C, D'Herbès JM. 1999. Niger tiger bush as a natural water harvesting system. Catena 37(1): 231-256. DOI: https://doi.org/10.1016/S0341-8162(98)00061-7

Van Auken OW. 2000. Shrub invasions of North American semiarid grasslands. Annual review of ecology and systematics 31(1): 197-215.

Wang X, Li X, Xiao H, Berndtsson R, Pan Y. 2007. Effects of surface characteristics on infiltration

patterns in an and shrub desert. Hydrological Processes 21(1): 72-79. DOI: 10.1002/hyp.6185

Weltzin JF, Loik ME, Schwinning S, Williams DG, Fay PA, Haddad BM, Harte J, Huxman TE, Knapp AK, Lin G, Pockman WT, Shaw RM, Small EE, Smith MD, Smith SD, Tissue DT, Zak JC. 2003. Assessing the Response of Terrestrial Ecosystems to Potential Changes in Precipitation. Bioscience 53(10): 941-952. DOI: 10.1641/0006-3568(2003)053[0941:ATROTE]2.0.CO;2

Wilcox BP, Breshears DD, Allen CD. 2003. Ecohydrology of a resource-conserving semiarid woodland: effects of scale and disturbance. Ecological Monographs 73(2): 223-239. DOI: 10.1890/0012-9615(2003)073[0223:EOARSW]2.0.CO;2

Yan M, Zuo H, Wang H, Dong Z, Li G. 2019. Snow resisting capacity of Caragana microphylla and Achnatherum splendens in a typical steppe region of Inner Mongolia, China. Journal of Arid Land. DOI: 10.1007/s40333-019-0021-x

Yang Y, Liu L, Shi P, Zhao M, Dai J, Lyu Y, Zhang G, Zuo X, Jia Q, Liu Y, Liu Y. 2019. Converging Effects of Shrubs on Shadow Dune Formation and Sand Trapping. Journal of Geophysical Research-Earth Surface 124(7): 1835-1853. DOI: 10.1029/2018JF004695

Zhang S, Li X, Jiang Z, Li D, Lin H. 2018. Modelling of rainfall partitioning by a deciduous shrub using a variable parameters Gash model. Ecohydrology 11(7): e2011. DOI: 10.1002/eco.2011

Zhang S, Li X, Peng H, Zhang Z. 2012. Infiltration pattern beneath shrub canopy and interspace grass patches in typical steppe ecosystems of Inner Mongolia, China. Journal of Earth Environment 3(6):

1117-1125.

Zhang S, Li X. 2018. Soil moisture and temperature dynamics in typical alpine ecosystems: a continuous multi-depth measurements-based analysis from the Qinghai-Tibet Plateau, China. Hydrology Research 49(1): 194-209. DOI: 10.2166/nh.2017.215

Zhang Z, Li X, Yang X, Shi Y, Zhang S, Jiang Z. 2019. Changes in soil properties following shrub encroachment in the semiarid Inner Mongolian grasslands of China. Soil Science and Plant Nutrition: 1-10. DOI: 10.1080/00380768.2019.1706430

Zhang Z, Wang S, Nyren P, Jiang G. 2006. Morphological and reproductive response of Caragana microphylla to different stocking rates. Journal of Arid Environments 67(4): 671-677.

Zheng X, Li X, Li L, Peng H, Zhang S. 2015a. Relationship and response of shrub patches to precipitation using the entropy model in arid and semiarid regions of China. Acta Ecologica Sinica 35(23): 7803-7811. (In Chinese with English abstract)

Zheng X, Zhao G, Li X, Li L, Wu H, Zhang S, Zhang Z. 2015b. Application of stable hydrogen isotope in study of water sources for Caragana microphylla bushland in Nei Mongol. Chinese Journal of Plant Ecology 39(2): 184-196. (In Chinese with English abstract)

Zhou L, Shen H, Chen L, Li H, Zhang P, Zhao X, Liu T, Liu S, Xing A, Hu H, Fang J. 2019. Ecological consequences of shrub encroachment in the grasslands of northern China. Landscape Ecology 34(1): 119-130. DOI: 10.1007/s10980-018-0749-2

615 **Table:**

616 Table 1 Preferential flow (PF) characteristics of different sites.

Sites	Period			Rain events		PF events					PF ratio (%)				
	Begin	End	Days	Total	> 1 mm	20 cm	40 cm	60 cm	100 cm	Total	20 cm	40 cm	60 cm	100 cm	Total
Top grass	Jul. 1, 2009	May 16, 2011	684	76	54	0	0	0	0	0	0.0	0.0	0.0	0.0	0.0
Top shrub	Aug. 1, 2009	May 16, 2011	653	70	49	0	0	0	0	0	0.0	0.0	0.0	0.0	0.0
Upper grass	Jul. 1, 2009	May 16, 2011	684	76	54	1	0	0	0	1	1.9	0.0	0.0	0.0	1.9
Upper shrub	Jul. 17, 2009	May 16, 2011	668	75	53	0	1	1	0	2	0.0	1.9	1.9	0.0	3.8
Middle grass	Jul. 1, 2009	May 21, 2013	1420	163	109	1	3	3	-	7	0.9	2.8	2.8	-	6.4
Middle shrub	Jul. 1, 2009	May 21, 2013	1420	163	109	1	1	2	-	4	0.9	0.9	1.8	-	3.7
Lower grass	Aug. 1, 2009	May 16, 2011	653	70	49	0	0	4	0	4	0.0	0.0	8.2	0.0	8.2
Lower shrub*	Jul. 1, 2009	May 16, 2011	543	70	51	0	1	0	0	1	0.0	2.0	0.0	0.0	2.0
Grass						2	3	7	0	12	0.7	0.7	2.7	0.0	4.1
Shrub						1	3	3	0	7	0.2	1.2	0.9	0.0	2.4

617 *missing period: Nov.1, 2009 - Mar. 21, 2010

618

619 Figures:

620 Figure 1 Diagrammatic sketch of the experimental hillslope with *C.*
621 *microphylla* patches interspersed in sparse grass matrix, and sites for soil
622 moisture sensors and meteorological tower instrumentation.

623 Figure 2 Meltwater infiltration estimation. Soil water storage (*SWS*, back
624 line), and soil temperature (red line) crossing soil frozen and the first rain
625 after soil thawed were given. The red dash line shows 0 °C. Black dot lines
626 show the frozen soil period. The green dot line shows *the* SWS just before
627 soil frozen and thawed. The blue dot line shows the maximum *of* SWS after
628 soil thawed and before the first rain.

629 Figure 3 Characteristics of rainfalls at the experimental area from July 1,
630 2009 to May 21, 2013. The grey solid line shows the density of rainfall
631 amount and the grey vertical lines show the occurs of rainfall events;
632 yellow columns show the count of rainfall events; the blue dash line shows
633 the cumulative percent of rainfall amount; the blue bubbles show the
634 rainfall amount, rainfall duration, and their sizes show rainfall intensity.

635 Figure 4 Wind speeds and direction in January, February, March,
636 November, and December of the experimental period at 3 m above the
637 middle of the slope.
638 Figure 5 The relationships between the changes of soil water storage
639 (ΔSWS) and rainfall amounts (P).
640 Figure 6 Yearly rainfall infiltration at different sites in 2009 and 2010.
641 Rainfall infiltration in 2009 were since July 1 except the top shrub site and
642 the lower grass site, which were since August 1, 2009.
643 Figure 7 The meltwater infiltration at different sites and periods.
644 Figure 8 Meltwater infiltration at the middle site in the period of 2012 -
645 2013. (a) Rainfall and air temperature (*Ta*) at 2 m above ground; (b) soil
646 water storage (*SWS*) and soil temperature at 10 cm depth at the middle
647 shrub site; (c) soil water content (θ) at 10, 20, 40, and 60 cm depth at the
648 middle shrub site; (d) soil water storage (*SWS*) and soil temperature at 10
649 cm depth at the middle grass site; (c) soil water content (θ) at 10, 20, 40,
650 and 60 cm depth at the middle grass site.
651 Figure 9 Photo of meltwater flow on the slope. Photo taken on March 7,
652 2011. Snow and ice were retained at the lee side of the shrub patch and

melted at the south first. Note that there were snow and ice on the shrub mound earlier than the time of this photo taken, and they melt earlier due to the stems of shrub had lower albedo and could absorbed more radiation. Photo courtesy of Si-Yi Zhang.

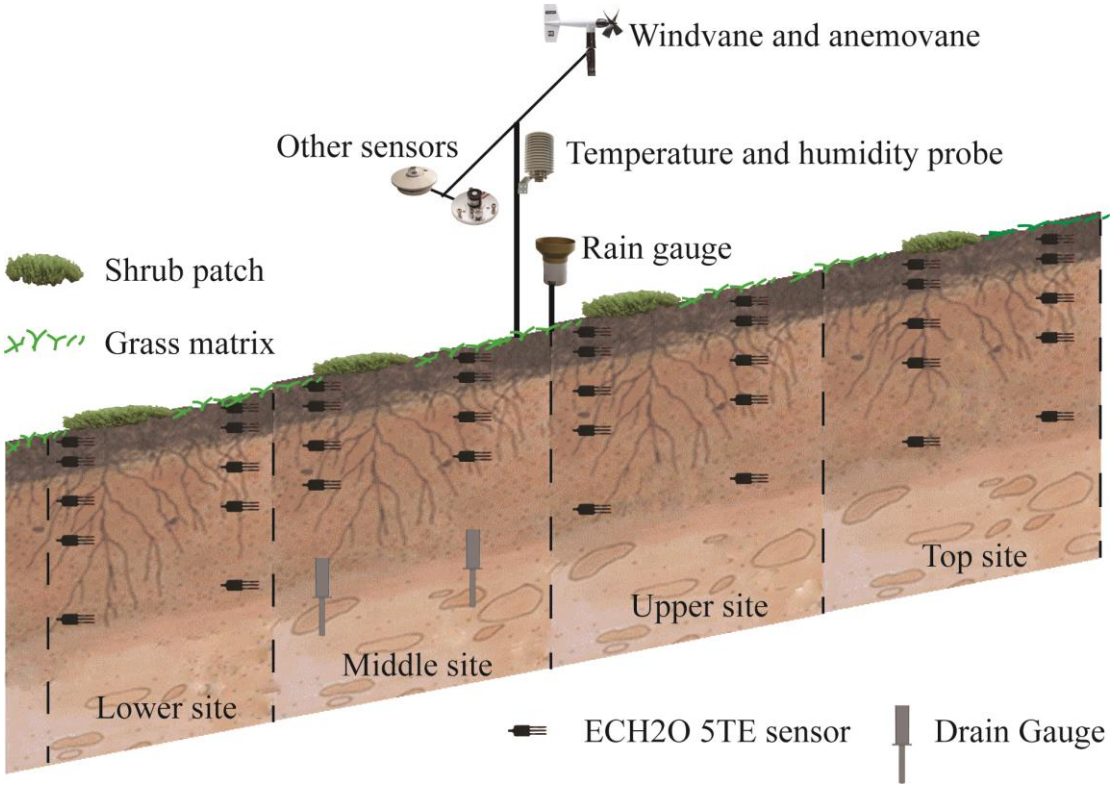

657

658 Figure 1 Diagrammatic sketch of the experimental hillslope with *C.*

659 *microphylla* patches interspersed in sparse grass matrix, and sites for soil

660 moisture sensors and meteorological tower instrumentation.

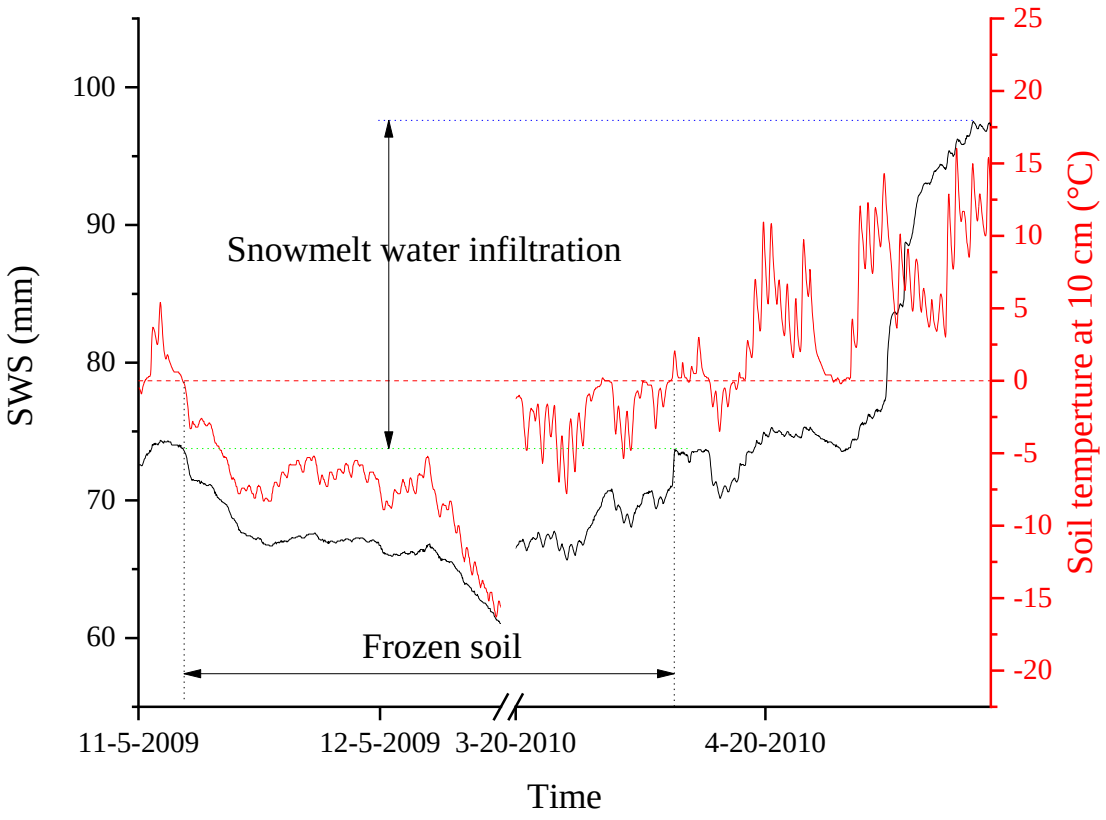

Figure 2 Meltwater infiltration estimation. Soil water storage (*SWS*, back line), and soil temperature (red line) crossing soil frozen and the first rain after soil thawed were given. The red dash line shows 0 °C. Black dot lines show the frozen soil period. The green dot line shows the *SWS* just before soil frozen and thawed. The blue dot line shows the maximum of *SWS* after soil thawed and before the first rain.

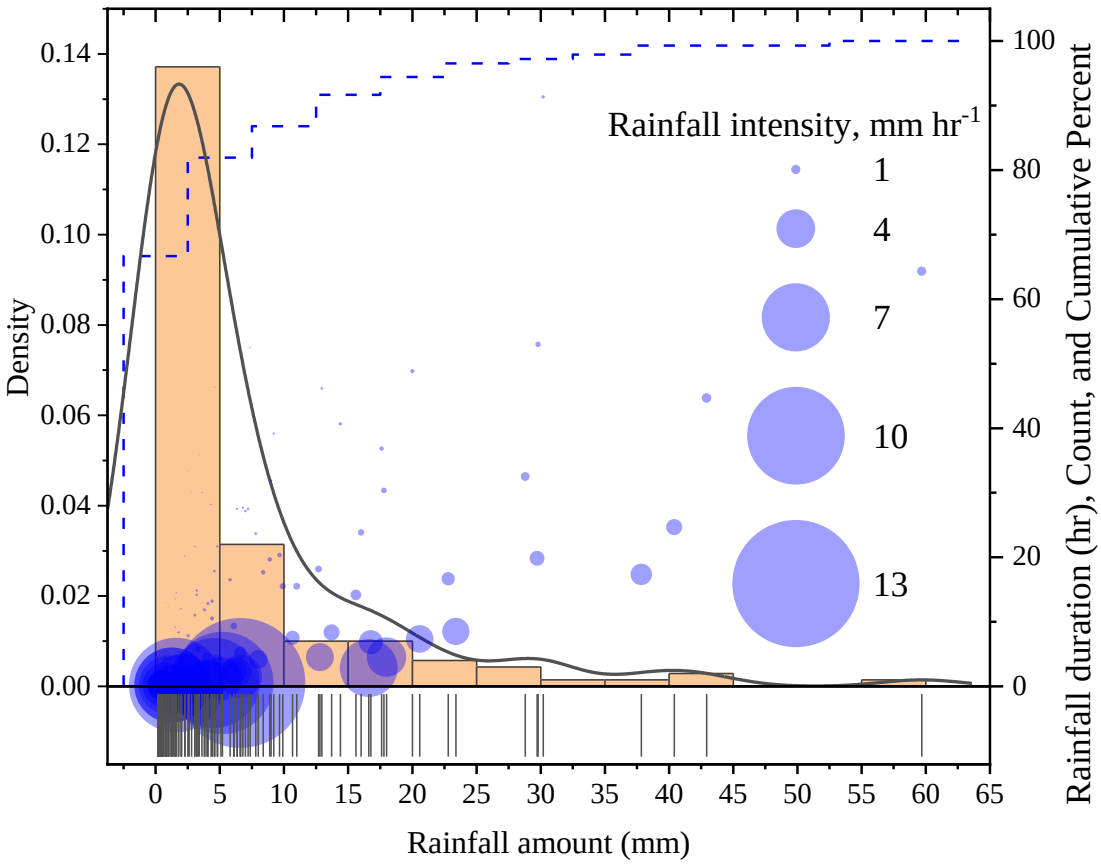

668

669 Figure 3 Characteristics of rainfalls at the experimental area from July 1,

670 2009 to May 21, 2013. The grey solid line shows the density of rainfall

671 amount and the grey vertical lines show the occurs of rainfall events;

672 yellow columns show the count of rainfall events; the blue dash line shows

673 the cumulative percent of rainfall amount; the blue bubbles show the

674 rainfall amount, rainfall duration, and their sizes show rainfall intensity.

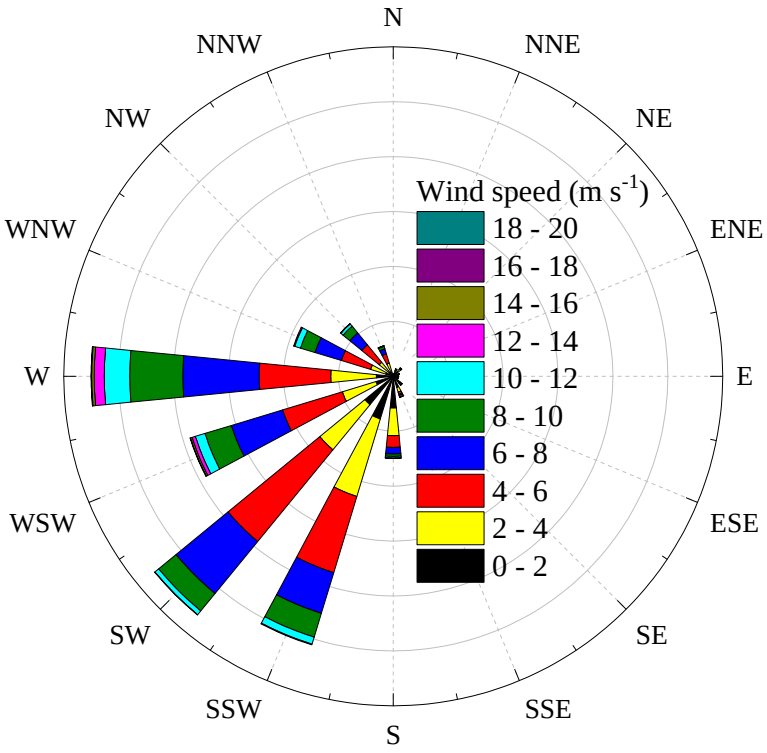

675

676 Figure 4 Wind speeds and direction in January, February, March,

677 November, and December of the experimental period at 3 m above the

678 middle of the slope.

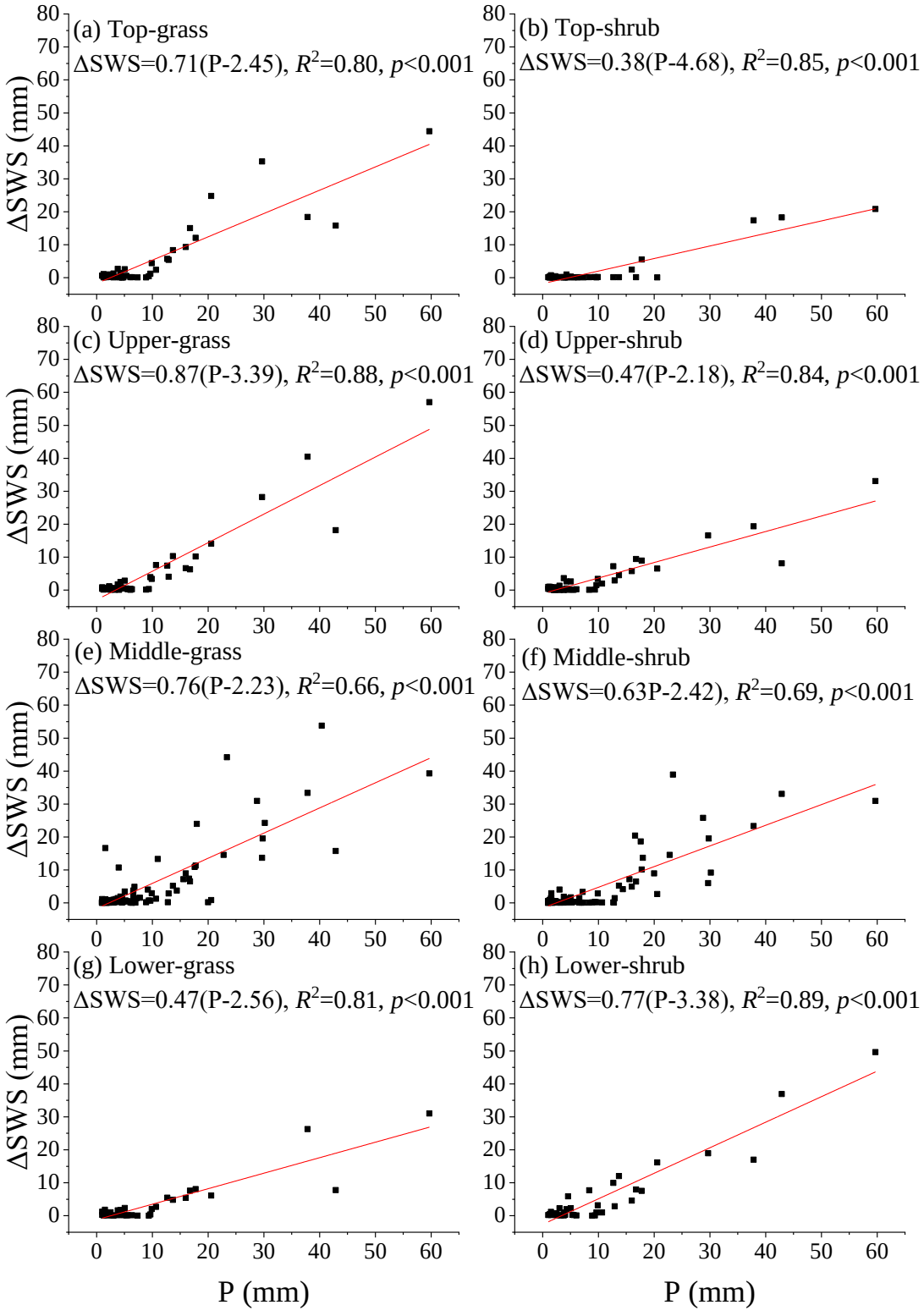

679

680 Figure 5 The relationships between the changes of soil water storage

681 (Δ*SWS*) and rainfall amounts (P).

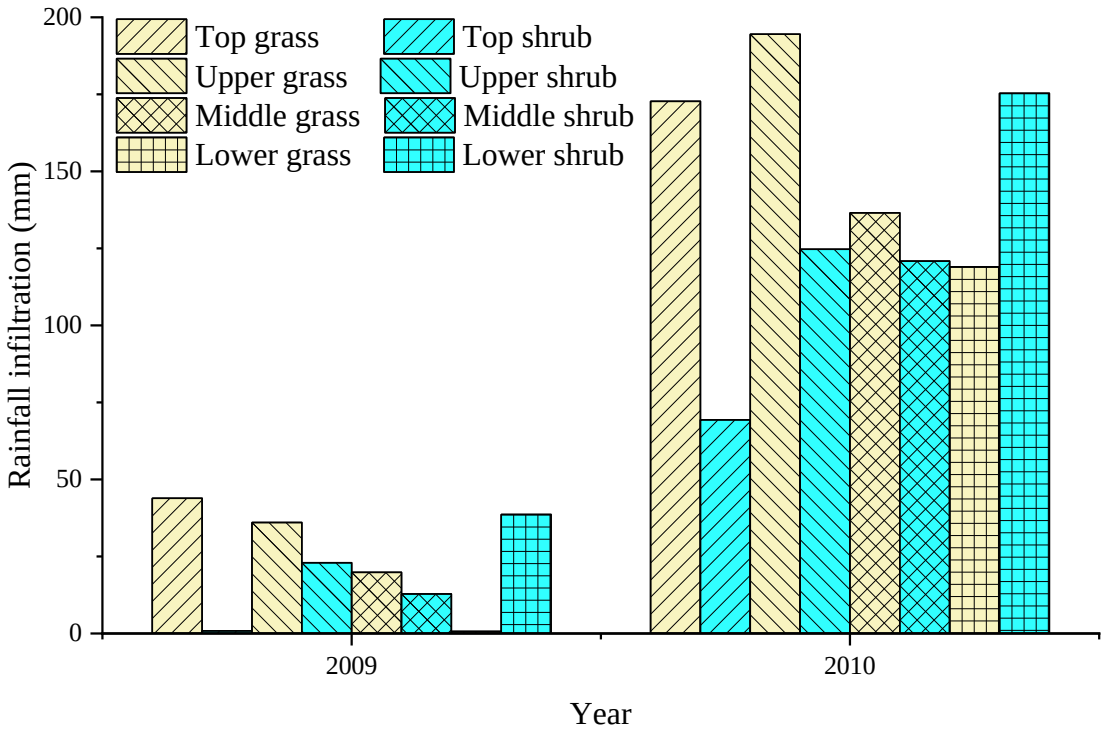

682

683 Figure 6 Yearly rainfall infiltration at different sites in 2009 and 2010.

684 Rainfall infiltration in 2009 were since July 1 except the top shrub site and

685 the lower grass site, which were since August 1, 2009.

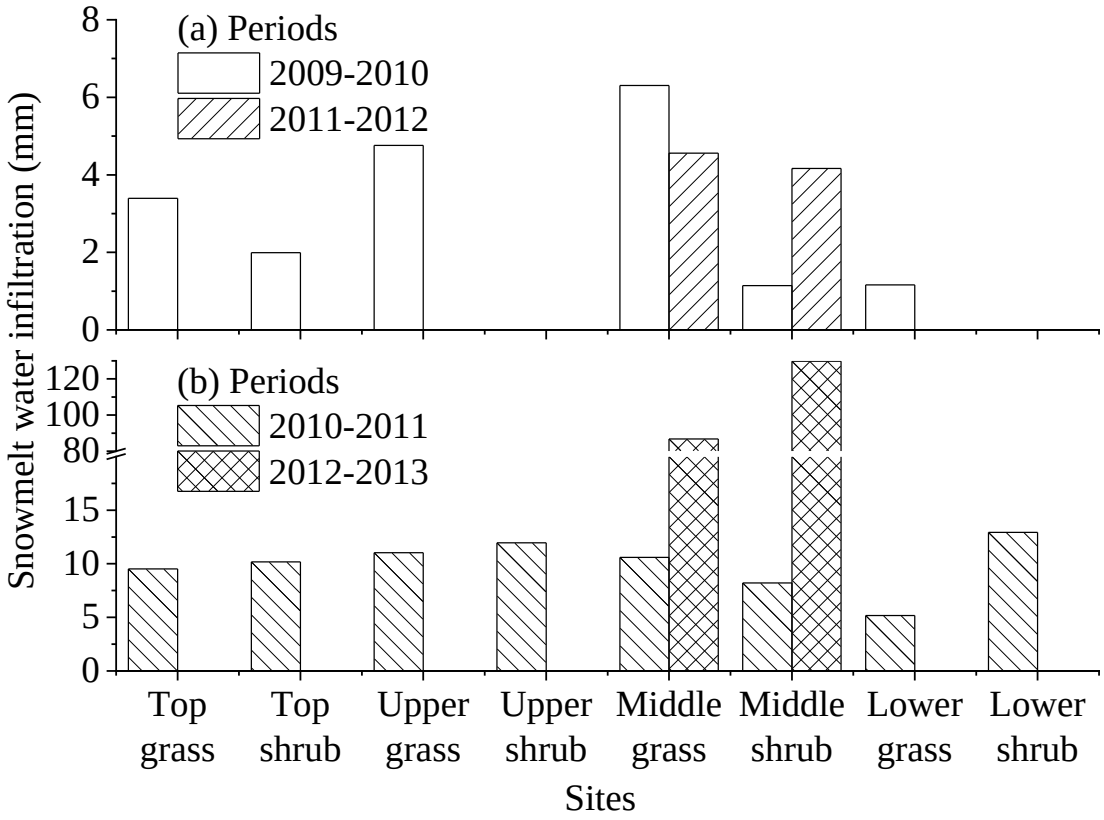

686

687 Figure 7 The meltwater infiltration at different sites and periods.

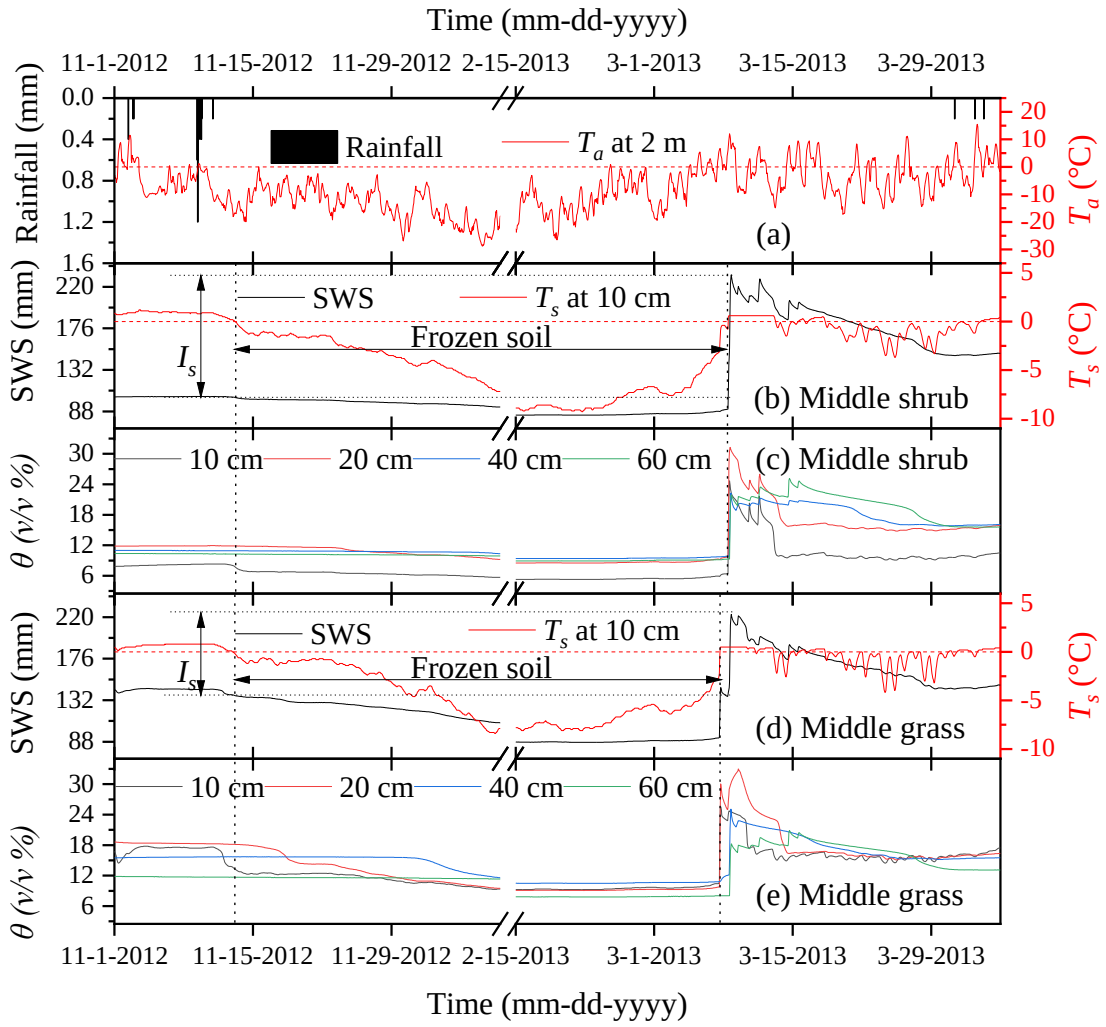

Figure 8 Meltwater infiltration at the middle site in the period of 2012 - 2013. (a) Rainfall and air temperature (T_a) at 2 m above ground; (b) soil water storage (*SWS*) and soil temperature at 10 cm depth at the middle shrub site; (c) soil water content (θ) at 10, 20, 40, and 60 cm depth at the middle shrub site; (d) soil water storage (*SWS*) and soil temperature at 10 cm depth at the middle grass site; (c) soil water content (θ) at 10, 20, 40, and 60 cm depth at the middle grass site.

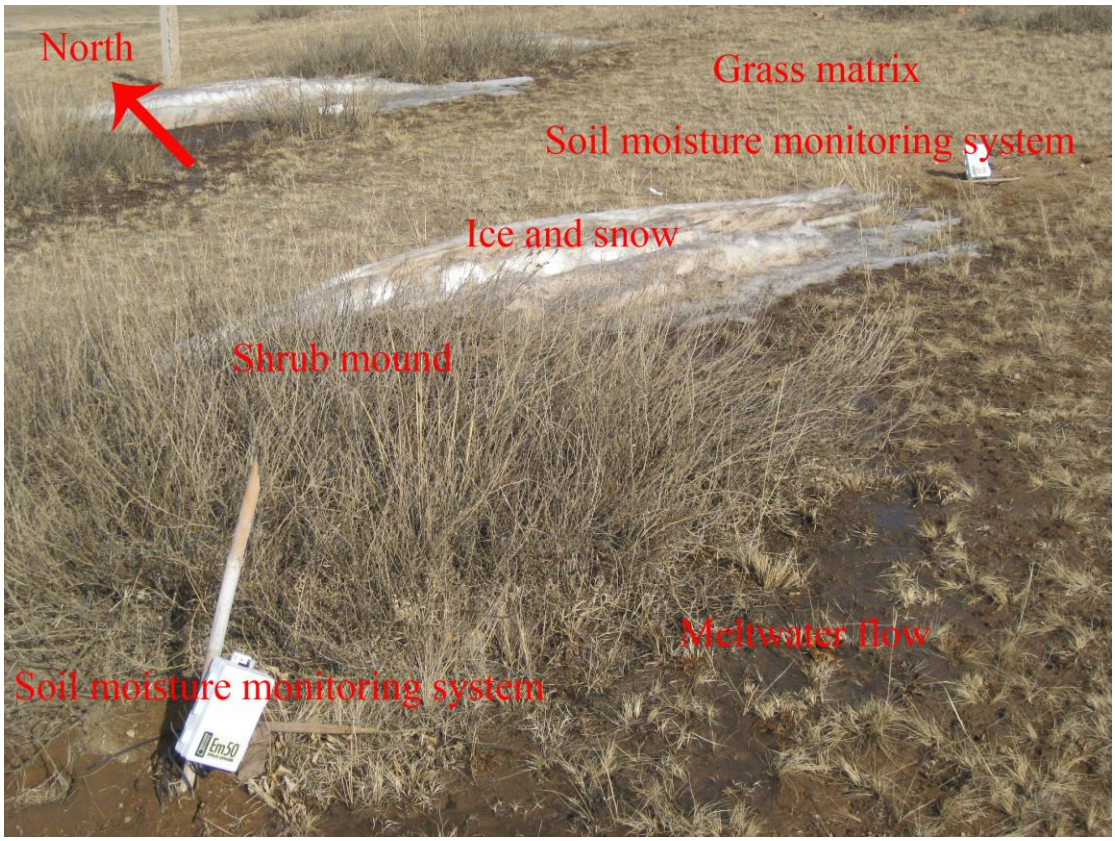

Figure 9 Photo of meltwater flow on the slope. Photo taken on March 7, 2011. Snow and ice were retained at the lee side of the shrub patch and melted at the south first. Note that there were snow and ice on the shrub mound earlier than the time of this photo taken, and they melt earlier due to the stems of shrub had lower albedo and could absorbed more radiation. Photo courtesy of Si-Yi Zhang.